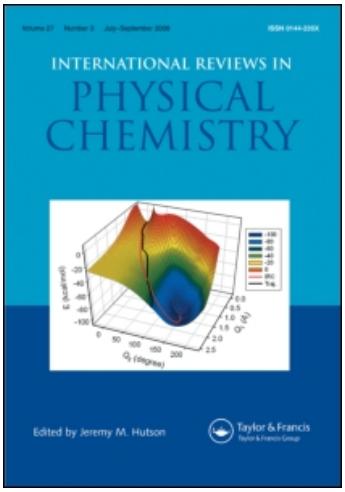


**International Reviews in Physical Chemistry**
Publication details, including instructions for authors and subscription information:
http://www.informaworld.com/smpp/title~content=t713724383

# Light-induced kinetic effects in molecular gases

L. J. F. Hermans[a]
[a] Huygens Laboratory, Leiden University, Leiden, The Netherlands

**To cite this Article** Hermans, L. J. F.(1992) 'Light-induced kinetic effects in molecular gases', International Reviews in Physical Chemistry, 11: 2, 289 — 315
**To link to this Article: DOI:** 10.1080/01442359209353273
**URL:** http://dx.doi.org/10.1080/01442359209353273

INTERNATIONAL REVIEWS IN PHYSICAL CHEMISTRY, 1992, VOL. 11, NO. 2, 289–315

# Light-induced kinetic effects in molecular gases

by L. J. F. HERMANS
Huygens Laboratory, Leiden University,
P.O. Box 9504, 2300 RA Leiden, The Netherlands

Velocity-selective excitation can be achieved by tuning a narrow-band laser within the Doppler-broadened absorption profile of a gas. If the excitation modifies the kinetic properties of the molecules (e.g., the kinetic cross-sections or the molecule–surface interactions), the Maxwell velocity distribution will be distorted. This gives rise to a new class of kinetic effects that do not require external gradients to be imposed on the system; rather, the laser intensity and its gradient can be considered as thermodynamic forces. Examples are light-induced drift, surface light-induced drift and light-induced viscous flow. A phenomenological overview is given of the various light-induced kinetic effects which can arise in pure gases or mixtures. This includes effects resulting from velocity-selective excitation immediately followed by collisional de-excitation ('velocity-selective heating'). The theoretical description of the various effects is briefly reviewed. Experiments are described which investigate these effects in molecular systems, where the excitation is rovibrational, and their results discussed. So far, data have been obtained for $CH_3F$, $NH_3$, $CO_2$, OCS, $CH_3OH$, $CH_3Br$, $SF_6$ and $C_2H_4$. Applications include determination of the vibrational-state dependence of intermolecular potentials, dependence of molecule–surface interactions upon the rotational state $(J, M_J)$, isotope separation, ortho–para conversion rates and possible astrophysical applications.



## 1. Introduction

The advent of narrow-band tunable lasers has given new impetus to the study of molecular collision processes. In the field of molecular beam experiments, it has especially proven possible to obtain detailed information on the collision dynamics of state-selected molecules, both in intermolecular scattering and in molecule–surface scattering. But tunable lasers have also been used to study collision processes in gas-cell type experiments, e.g. by Raman scattering or pressure broadening measurements. In most of these cases the laser is used as a purely diagnostic tool, or to prepare molecules in a specific state.

It was not until 1979 that it was realized (Gel'mukhanov and Shalagin 1979a) that tunable lasers can themselves bring about transport phenomena, even if the photon momentum is disregarded. Two requirements have to be met. First, the excitation process has to be velocity selective. This can be achieved by tuning the laser frequency within the Doppler broadened absorption profile, thereby exciting only those molecules which are Doppler shifted into resonance. For the simplified case of $\delta$-peak excitation one has $\omega_L - \omega_0 = kv_L$, where $\omega_L$ is the laser frequency, $\omega_0$ the optical transition frequency, $k(=2\pi/\lambda)$ the magnitude of the wave-vector and $v_L$ the laser-selected velocity component along the propagation direction of the laser light. The second requirement is that the excitation process must change the kinetic properties of the particles. This is usually the case since the excited molecules usually have a larger kinetic cross-section—or larger collision rate—than their ground-state counterparts. The combination of these two requirements, i.e., velocity-selective excitation and state-dependent interaction, will cause the gas to be kinetically anisotropic, and transport effects will occur.

0144-235X/92 $3·00 

One way to look at this is to consider the velocity distribution. This is illustrated in figure 1 for the case that the laser light propagates along the positive $x$ axis and is tuned slightly above resonance. Due to the excitation, a Bennett hole will be burned in the ground-state distribution and a corresponding Bennett peak will appear in the distribution of particles in the excited state. If the kinetic properties of ground-state and excited particles were identical, the two distributions would still add up to a Maxwellian distribution and the gas would remain in equilibrium. If, however, the kinetic cross-section $\sigma$ for the excited molecules differs from that for the ground-state molecules (i.e., $\sigma_e \neq \sigma_g$), this is no longer the case. If we assume $\sigma_e > \sigma_g$, the rate at which excited particles collide out of the velocity class around $v_L$ exceeds that at which ground-state particles collide into it: switching on the laser breaks detailed balance. Therefore, in the stationary state, the Bennett hole in $f_g$ will be slightly larger than the peak in $f_e$, and the total velocity distribution $f_g+f_e$ will still have a small net hole around $v_x=v_L$.

Notice that we have now directly manipulated the velocity distribution by optical means. This is in sharp contrast to the traditional indirect way of influencing the distribution function by applying external gradients of temperature, velocity or concentration.

One may be tempted to think that the case of a pure, light-absorbing gas forms the ideal playground for light-induced kinetic effects (LIKE), provided that the pressure is low enough to make the homogeneous linewidth small compared to the Doppler width and high enough to make boundary layer effects negligible. However, the conceptually easiest (and best studied) effect, light-induced drift (LID), cannot occur in a pure gas, since this is excluded by momentum conservation (this means that the total velocity distribution, despite the above discussed hole around $v_L$, is deformed in such a way that the first moment remains zero: $\int (f_g+f_e)v_x\,dv_x=0$). Therefore, in the overview of Section 2 we will first treat the two cases in which LID does occur, the necessary momentum being provided by a background buffer gas ('ordinary LID', Section 2.1) or

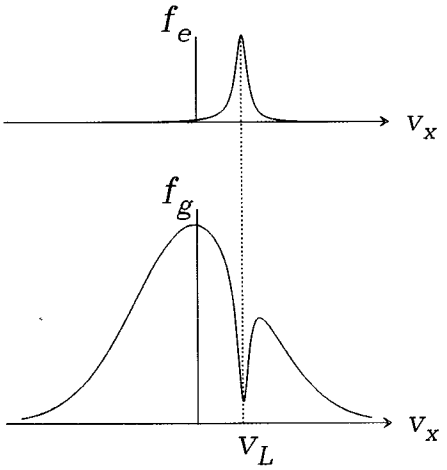


Figure 1. Excited-state and ground-state velocity distribution, $f_e(v_x)$ and $f_g(v_x)$, respectively, under velocity-selective excitation by laser radiation propagating along the $x$ axis and slighly detuned from resonance: $\omega_L-\omega_0=kv_L$. If the kinetic cross-sections in ground- and excited-state differ, the two distributions will not add up to a Maxwellian and transport effects will result.

by the wall of the containing vessel ('Surface LID', Section 2.2)). The more subtle effects arising in a pure gas from higher moments will be considered in Section 2.3. Additional effects arising only in a non-uniform laser field are treated in Section 2.4. Section 2.5 is devoted to a type of LIKE in which the condition of state-dependent interaction is somewhat relaxed. This type makes use of the combination of velocity-selective excitation and rapid collisional de-excitation. Such a combination gives rise to what may be called 'velocity-selective heating': molecules moving parallel to the $\boldsymbol{k}$ vector have a different mean kinetic energy than those moving anti-parallel. This creates an anisotropy in the transport properties, and therefore gas-kinetic effects, even in the case that the elastic cross-sections in excited- and ground-state are identical. In Section 2.6 some less well-known light-induced kinetic effects are briefly mentioned.

In Section 3 an overview of the theoretical and experimental results is given, with the emphasis on the experiments. It will be found that light-induced kinetics for molecular systems has developed into a rich field of research. In addition to producing some conceptually new phenomena, this field is found capable of yielding interesting information on the role of rotational and vibrational state in molecule–molecule or molecule–surface collision dynamics. One reason is that the experiments are differential by nature; their results are directly proportional to the difference in kinetic properties between ground-state and excited-state molecules, and the phenomena are absent if this difference vanishes. Therefore the experiments are sensitive for even subtle dependences of, e.g., the molecule–surface interaction upon the rotational state.

An explicit summary of applications of LIKE is given in Section 4.



## 2. Light-induced kinetic effects: overview

When making a systematic classification of the various effects it is useful to realize, as shown by Nienhuis (1989), that both the incident radiation and the gradient of its intensity can be considered as a thermodynamic force. In order to make a clear distinction between the two types, we will assume, in the first three cases to be treated below, that the radiation is essentially uniform: only a small intensity gradient along the propagation direction will be assumed to account for the absorption. In the subsequent cases, treated in Sections 2.4 and 2.5, an intensity gradient perpendicular to the propagation direction will be essential.

Throughout Section 2 we will make the simplifying assumption that we work in the Doppler limit: only a narrow velocity group around $v_x = v_L$ is excited ($\delta$-peak excitation). In practice this is achieved with a narrow-band laser and small homogeneous linewidth.

### 2.1. *Light-induced drift through a buffer gas*

If the light absorbing particles are immersed in a non-absorbing buffer gas, velocity-selective excitation can bring about LID. For two-level particles, this may be easily understood as follows. Due to collisions with the buffer gas, the distributions of particles in ground- and excited-states will thermalize. However, in general the kinetic cross-section of the excited state, $\sigma_e$, differs from that of the ground-state, $\sigma_g$. Usually one has $\sigma_e > \sigma_g$, see figure 2. In this case the rate of thermalization of the excited particles exceeds that of the ground-state particles. Alternatively, one may say that the diffusion coefficient of the excited particles is smaller than that of the ground-state particles, with respect to the buffer gas. This breaks the symmetry and, as a consequence, the

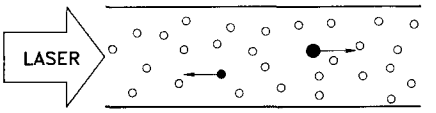


Figure 2. Principle of light-induced drift: velocity-selectively excited particles have (usually) a larger cross-section and hence a shorter mean free path than their ground-state counterparts. The resulting drift through the buffer gas (open circles) will give rise to a concentration gradient in a closed tube.

absorbing gas as a whole will drift in the direction opposite to that of the (larger) excited particles with a velocity given by:

$$v_{\mathrm{LID}} = -v_{\mathrm{L}} \frac{n_{\mathrm{e}}}{n_{\mathrm{a}}} \frac{\sigma_{\mathrm{e}} - \sigma_{\mathrm{g}}}{\sigma_{\mathrm{g}}}. \tag{1}$$

Here, $n_{\mathrm{e}}$ is the number density of excited particles which have not yet suffered a thermalizing collision (more precisely: $n_{\mathrm{e}} v_{\mathrm{L}}$ is the particle flux in the excited state), whereas $n_{\mathrm{a}} = n_{\mathrm{e}} + n_{\mathrm{g}}$ is the number density of absorbing particles; spontaneous decay is assumed to be slow. Although equation (1) has been more rigorously derived, e.g. by Gel'mukhanov and Shalagin (1979a), it follows already from the following qualitative argument. Let us assume that we excite $p$ particles per unit time and volume in a narrow velocity class around $v_x = v_{\mathrm{L}}$. If the average time between Maxwellizing collisions (assumed to be much longer than the radiative lifetime) is given by $\tau_{\mathrm{e}}$ in the excited and by $\tau_{\mathrm{g}}$ in the ground-state, the number density of non-thermalized excited particles is given by

$$n_{\mathrm{e}} = p\tau_{\mathrm{e}}. \tag{2}$$

These have now replaced ground-state particles in the velocity class around $v_{\mathrm{L}}$ whose number density would have been

$$n_{\mathrm{g}} = p\tau_{\mathrm{g}}. \tag{3}$$

The net flux resulting from this process is given by

$$j = n_{\mathrm{e}} v_{\mathrm{L}} - n_{\mathrm{g}} v_{\mathrm{L}} = n_{\mathrm{e}} v_{\mathrm{L}} \left( \frac{\tau_{\mathrm{e}} - \tau_{\mathrm{g}}}{\tau_{\mathrm{e}}} \right). \tag{4}$$

Upon substitution of $j = n_{\mathrm{a}} v_{\mathrm{LID}}$ and $\tau \propto \sigma^{-1}$, equation (1) is directly recovered. Alternatively, one can find equation (1) from an elementary argument based on one-dimensional random walk with unequal steps (Eliel 1992). As seen from equation (1), the drift velocity can have either sign, depending on the detuning $\omega_{\mathrm{L}} - \omega_0 = kv_{\mathrm{L}}$. This is in contrast to radiation pressure, which always produces a drift in the direction of the wave-vector. Since the excited-state density $n_{\mathrm{e}}$ follows the Gaussian absorption profile for weak absorption, the detuning behaviour is dispersion-curve-like (see figure 3). Due to momentum conservation the buffer gas will move in the opposite direction, resulting in a separation of the two components of the mixture.

LID was originally envisaged by its founding fathers (Gel'mukhanov and Shalagin 1979a) for the case of electronic excitation of an atomic vapour in a buffer gas. Since the change in collision cross-section can be up to 50% and the light absorption probability is large, LID can take spectacular forms in this case and lead to what has become known as the 'optical piston' (Werij *et al.* 1984). For a recent review of LID in atomic

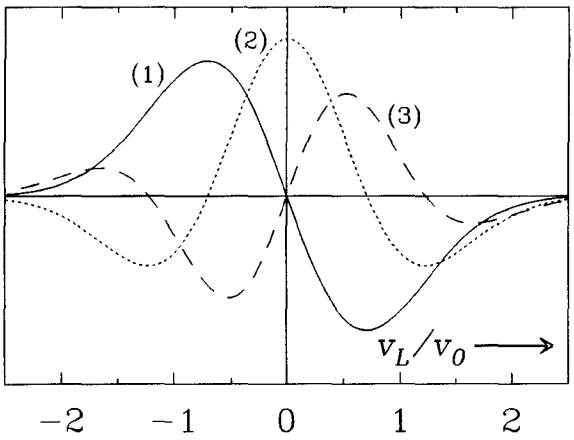


Figure 3. Typical detuning behaviour for various light-induced kinetic effects in a laser field having homogeneous intensity, for the case that the excited-state fraction $n_e/n$ follows a Gaussian absorption profile $\propto \exp(-v_L^2/v_0^2)$ and $\Delta\sigma/\sigma$ is constant. Curve (1) represents the first moment of the velocity, i.e., the drift velocity for LID and SLID (equations (1) and (5)), curve (2) the second moment, i.e., the light-induced pressure anisotropy (equation (6)), and curve (3) the light-induced heat flux (equation (7)). Note that curve (1) is the derivative of the absorption profile, while each higher-order curve is the derivative of the previous order (see also the corresponding equation).



systems the reader is referred to a review paper by Eliel (1992). Experimental results for molecular systems will be discussed in Section 3.1.

### 2.2. *Surface light-induced drift*

If the molecule–surface interaction is state dependent, a particle drift can occur along the wall of the containing vessel. This phenomenon is called surface light-induced drift (SLID). It is analogous to LID with the role of the buffer gas taken over by the wall. It therefore occurs in its purest form if the (one-component) gas is at such low pressure that molecule–surface collisions dominate, i.e., in a Knudsen gas. If the accommodation coefficient for tangential momentum transfer, $\alpha$, is state dependent, velocity-selective-excitation can give rise to net transfer of tangential momentum to the surface (see figure 4). This will result in a drift of the gas in the direction of the particles having the smallest accommodation:

$$v_{\mathrm{SLID}} = -v_{\mathrm{L}} \frac{n_{\mathrm{e}}}{n} \frac{\alpha_{\mathrm{e}} - \alpha_{\mathrm{g}}}{\alpha_{\mathrm{g}}}, \tag{5}$$

where $\alpha_e$ and $\alpha_g$ are the accommodation coefficients for tangential momentum transfer of the excited-state and ground-state molecules, respectively. As follows from the analogy between equations (1) and (5), the detuning behaviour is the same as for LID (see figure 3). Momentum conservation is not violated since the wall can be viewed as an infinite sink or source of momentum. Experimental results for the effect will be summarized in Section 3.2.

### 2.3. *Light-induced pressure anisotropy and light-induced heat flux*

In a pure gas at sufficiently high density such that molecule wall collisions can be neglected (mean free path $l \ll$ tube radius $R$) the particles collide only with particles of

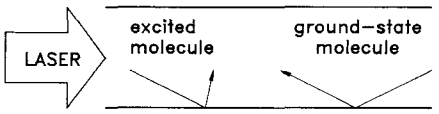


Figure 4. Principle of surface light-induced drift. The velocity- selectively-excited molecules are assumed to transfer a larger fraction of their tangential momentum to the surface than their ground-state counterparts, and a drift will result. In a closed tube this gives rise to a pressure difference $\delta p$ between the ends of the tube.

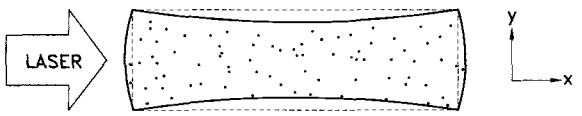


Figure 5. Visualization of the effect of light-induced pressure anisotropy in a cell having flexible walls (see equation (6)).



the same species. Also in this case a state-dependent collision cross-section gives rise to different thermalization rates for the ground-state and excited-state distributions (figure 1), leading to a net dip in the total distribution. Nevertheless, light-induced drift cannot occur since it is prevented by momentum conservation: the resulting non-equilibrium distribution must have a first moment equal to zero, i.e. $\langle v_x \rangle = 0$. However, in principle it should also be possible to observe new effects which arise from higher moments of the total distribution function, as was first pointed out by Folin *et al.* (1981) and treated formally by Nienhuis (1989). A non-equilibrium second moment gives rise to light-induced pressure anisotropy, whereas a non-zero third moment corresponds to a light-induced heat flux.

The occurrence of light-induced pressure anisotropy can be understood as follows. Let the laser be tuned on exact resonance of the transition so that the net dip in the total distribution function will be located around $v_x = 0$. Because of particle conservation, the higher $|v_x|$ values will become overpopulated. This results in $\langle v_x^2 \rangle > \langle v_x^2 \rangle_{eq}$ and therefore in an increase in the $xx$ component of the pressure tensor, i.e., a higher pressure 'in the $x$ direction'. Due to energy conservation, this increase must be at the expense of the other diagonal elements of the pressure tensor: in the $y$ and $z$ directions a pressure decrease will occur being half the pressure increase in the $x$ direction (see figure 5). If the laser is tuned in the far Doppler wings, the reverse process will take place and the effect changes sign. An expression for the pressure anisotropy, $p_{xx} - p_{yy} = p_{xx} - p_{zz}$, arising from velocity-selective excitation is given by Folin *et al.* (1981) and by Nienhuis (1989):

$$\frac{p_{xx} - p_{yy}}{p} = +\frac{n_e}{n}\frac{\Delta\sigma}{\sigma}\left[1 - 2\left(\frac{v_L}{v_0}\right)^2\right]. \tag{6}$$

Here $p = \frac{1}{3}(p_{xx} + p_{yy} + p_{zz})$ is the isotropic pressure, and $v_0 = (2k_B T/m)^{1/2}$ the thermal velocity. The detuning behaviour following from equation (6) is sketched in figure 3. Note that the pressure anisotropy is even in detuning.

The light-induced heat flux discussed here arises from the fact that under velocity-selective excitation with a state-dependent kinetic cross-section, the resulting a symmetric velocity distribution can have a non-vanishing third moment, i.e.,

$\langle v_x v_x^2 \rangle \neq 0$. This effect was treated theoretically by Folin *et al.* (1981) and by Nienhuis (1989). The resulting expression for the light-induced heat flux reads:

$$q_x = \frac{3}{2} p \frac{n_e}{n} \frac{\Delta\sigma}{\sigma} v_L \left[ 1 - \frac{2}{3} \left( \frac{v_L}{v_0} \right)^2 \right]. \tag{7}$$

The detuning behaviour is shown in figure 3.

For sake of completeness we note that contributions to the pressure anisotropy as well as to the heat flux arise also from spatial gradients of the light intensity (Nienhuis 1989). These contributions (which have a detuning behaviour different from that given in figure 3) arise as first-order effects in the systematic treatment by Nienhuis. Therefore, they are smaller than the zero-order effects of equations (6) and (7) by typically a factor $l/R$. Hence they may be neglected here since we have assumed $l/R \ll 1$.

### 2.4. *Light-induced viscous flow*

This effect has the gradient of the light intensity as the driving force. It can occur (and has been measured) in both pure gases and gas mixtures. At first glance, one may not expect a light-induced flow in a pure gas, being excluded by momentum conservation if the wall does not play an active role. However, if the light intensity varies over the cross-section of the beam (which is usually the case), the gas will be set into motion by the following mechanism. Let us assume that velocity-selective excitation increases the collision cross-section of particles travelling with a certain $x$ velocity. Due to the increased cross-section these particles transport their momentum less efficiently in the radial direction than do their ground-state counterparts. Since the illumination of the tube is non-uniform, this will result in a net transport of $x$ momentum in the radial direction, i.e., a stress in the gas will be produced. This, in turn, will give rise to a non-uniform flow velocity in the tube. For a specularly reflecting surface, momentum conservation would still require a vanishing particle flux when averaged over the cross-section of the tube. For real surfaces, however, most of the $x$ momentum will be absorbed by the wall, resulting in a net flow of the total gas. For the traditional stick-boundary-condition (where the velocity near the wall is assumed to be zero) and under the assumption that the light intensity vanishes near the wall, one finds:

$$v_{\mathrm{LIVF}}(r) = \frac{\pi}{2} v_L \frac{\Delta\sigma}{\sigma} \frac{n_e(r)}{n}. \tag{8}$$

This effect is called light-induced viscous flow (LIVF). In a closed tube, this flow will give rise to a pressure difference in the steady-state. Its detuning behaviour is identical to that for LID (curve (1) in figure 3), as can be seen from equation (8). Further details and experimental results will be given in Section 3.4.

### 2.5. *Velocity-selective heating/cooling as a source for LIKE*

As far as the effects treated above have their origin in the bulk of the gas, their primary cause is the state-dependent cross-section. This may be interpreted as a difference in the transport coefficients between excited-state and ground-state molecules. However, the transport coefficients can also be changed by changing the mean thermal speed of the particles. In order to achieve this for a selected velocity group only ('velocity-selective heating'), the mechanism of inelastic collisions can be invoked as an intermediate step. Let us consider a group of velocity-selectively excited molecules

which transfer part of their excitation energy into kinetic energy during the first collision. This will make both collision partners 'hotter' and thus increase their contribution to the transport properties (see figure 6).

The effect of the enhanced transport properties under velocity-selective heating is most conveniently studied for the case of momentum transport in a pure gas. For non-uniform illumination, a situation arises which is quite analogous to LIVF discussed above. This is illustrated in figure 7. For the velocity-selective heating process, rotational de-excitation is an effective mechanism, since this occurs on the time scale of a kinetic collision. Vibrational de-excitation may be disregarded since this occurs at time scales larger by a factor of $10^3$ to $10^4$ for most molecules. Let us assume that the rotational energy $\Delta E_{\text{rot}}$ picked up by a molecule from the laser field is, at the first collision after excitation, converted into kinetic energy with a probability $f$. This will make both the de-exciting molecule and its collision partner 'hotter' by $\Delta T = \frac{1}{2} f \Delta E_{\text{rot}} / \frac{3}{2} k_{\text{B}}$ on the average. The corresponding increase in thermal velocity $\bar{v}$ will enhance the transport of the selected momentum $mv_{\text{L}}$ (shared by the two molecules) relative to that of its counterpart $-mv_{\text{L}}$ (see figure 7 (*a*)). This does not yet produce a net momentum transport in the $y$ or $z$ direction if the illumination of the tube is spatially homogeneous. If, however, the illumination is inhomogeneous, a net stress will result (see figure 7 (*b*)). In analogy with the LIVF discussed in Section 2.4 this will produce a flow profile in an open tube and a pressure difference in a closed tube (figure 7 (*c*)).

The increase in thermal velocity discussed above would be the only contribution to this effect if the molecules were perfectly hard spheres. For realistic molecules, however, the cross-section decreases—and thus the mean free path $l$ increases—for increasing relative velocity. Thus, it is the increase in the product $\bar{v}l$ which determines the magnitude of this effect. The relative change in this product with changing temperature can be directly derived from the temperature dependence of the relevant transport coefficient, i.e., the viscosity $\eta$. This is most easily seen by considering the mean-free-path expression, $\eta \approx \frac{1}{3} \bar{v} l \rho$, with $\rho$ the mass density. Consequently, one expects this phenomenon to be determined by $\Delta(l\bar{v})/(l\bar{v}) = \Delta\eta/\eta$. Using the expression for $\Delta T$ derived above, one finds

$$\frac{\Delta\eta}{\eta} = \frac{1}{\eta} \frac{\mathrm{d}\eta}{\mathrm{d}T} \frac{f \Delta E_{\text{rot}}}{3k_{\text{B}}}. \tag{9}$$

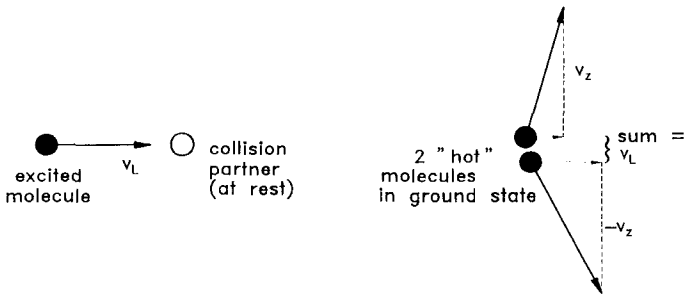


Figure 6. The principle of 'velocity-selective heating' schematically. (*a*) An optically excited molecule having velocity $v_{\text{L}}$ along the propagation direction of the light collides with a ground-state collision partner (assumed at rest). If the photon energy is converted into kinetic energy in the collision (*b*), both collision partners, now in the ground state, will have increased thermal speed, sharing the initial momentum $mv_{\text{L}}$.

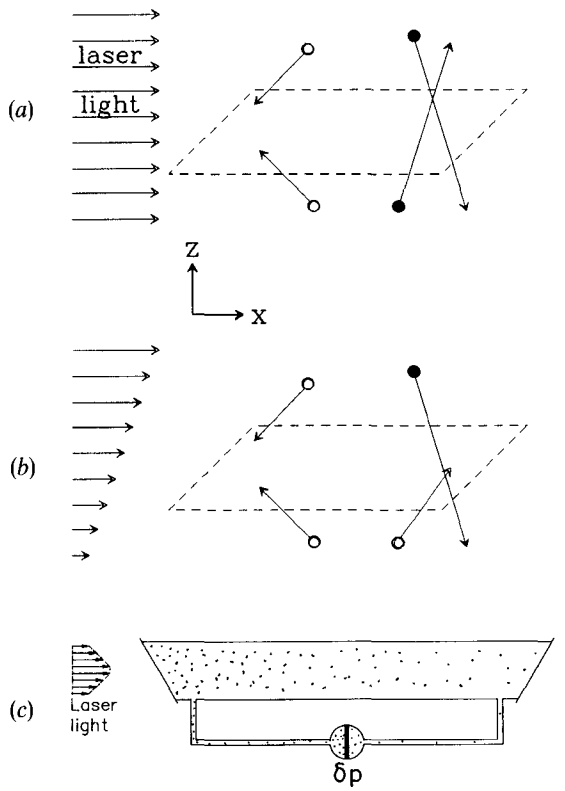


Figure 7. Light-induced viscous flow resulting from velocity-selective heating. (*a*) Due to increased thermal speed upon de-excitation (figure 6), molecules carrying the momentum $mv_L$ have enhanced momentum transport in the transverse ($z$) direction relative to those carrying $-v_L$. (*b*) In the case of non-uniform illumination this produces a stress. The resulting velocity profile, anchored at the boundary, gives a net flow through a tube. (*c*) In the experiment this is measured as a pressure difference in a closed tube (length $L = 300$ mm, radius $R = 0{\cdot}75$ mm).

Therefore, in this simplified picture one expects that the quantity $-\Delta\eta/\eta$ should replace the quantity $+\Delta\sigma/\sigma$ in expression (8) to make it apply to the present effect.

As pointed out above, the vibrational part of the energy in ro-vibrational excitation can be generally disregarded for this effect. Since the rotational part can have either sign (P against R-branch transitions), one may achieve both 'velocity-selective heating' and 'cooling' by selecting the proper transition. Evidence for such an effect was found by Hoogeveen and Hermans (1990). Further results will be given in Section 3.5.

### 2.6. *Other light-induced kinetic effects*

In this subsection we will briefly mention various other forms of LIKE which seem to have escaped the attention of experimentalists so far.

Polarization of a dipolar gas by LID was treated by Gel'mukhanov and Il'ichov (1983). They show that polar molecules should become oriented during their drift through a buffer gas and that an electric field will result.

A form of drift which does not depend on state-dependent collision rates with respect to the buffer gas was discussed by Levin (1981) and by Vaksman (1984). For the

case where the concentration of active particles is very much larger than that of the buffer gas, the velocity distribution of the former is distorted by a state-dependent collision rate for collisions between the active particles themselves. This sets the buffer gas into motion and—due to momentum conservation—also the active species.

A special case in which a flow profile in a one-component gas can be caused by a radiation field, even if this is spatially homogeneous, was treated by Folin and Komarov (1980). These authors considered the situation in which a plane parallel cell is placed under an angle with the $\boldsymbol{k}$ vector of the exciting laser light. Making use of the pressure anisotropy discussed in Section 2.3 they noted that, even at precise resonance ($v_L = 0$), a flow profile is set-up if the walls are assumed to cause specular reflection.

Sound generation by periodic velocity-selective excitation is another form of LIKE. This was treated theoretically by Gel'mukhanov (1984a, b). In order to distinguish this mechanism from ordinary opto-acoustics, one can modulate the detuning rather than the intensity of the radiation field. Note that in this method of sound generation, the acoustic energy is drawn from the thermal energy of the gas rather than from the photon energy.

Excitation of molecules by circularly or linearly polarized light creates anisotropic M-state distributions corresponding to orientation and alignment. If the excitation is velocity selective and a buffer gas is added, new light-induced kinetic effects can arise in addition to LID itself. As discussed by Gel'mukhanov and Il'ichov (1985a), circularly polarized light produces a rotation in the gas similar to the Magnus force, while linearly polarized light produces an anisotropic friction force on the aligned particles. The special case of particles lacking inversion symmetry (stereoisomers or chiral molecules) was treated by Il'ichov (1985). For such molecules, orientation can also be the results of their drift through a buffer gas, whether or not the light producing the drift is polarized. This phenomenon was theoretically treated by Gel'mukhanov and Il'ichov (1985b).



## 3. Results of theory and experiment

Most of the phenomena discussed in Sections 2.1–2.5 have been experimentally investigated in molecular gases. This is in contrast to the situation for atomic systems, where the experiments have been limited so far to LID through a buffer gas. The main reason is the extremely low vapour pressure of the experimentally most attractive atomic species, Na and Rb. An extensive survey of LID for atomic vapours was recently given by Eliel (1992). The primary goal of this Section is, therefore, to survey the experimental work on LIKE in molecular systems. This will be preceded, for each effect, by a brief sketch of the development of the theory, to help the interesting reader find his way through the vast literature.

After the prediction of LID by Gel'mukhanov and Shalagin (1979a) and the first experimental demonstration for Na–noble gases by the same group (Antsygin *et al.* 1979), most of the early theoretical work on LIKE was devoted to the description of LID. Various collision models were used to describe the collisions between the light-absorbing particles and the buffer gas, e.g., by Dykhne and Starostin (1980), Mironenko and Shalagin (1981), Lawandy (1983), Berman *et al.* (1986), Kryszewski and Nienhuis (1987, 1989).

A convenient model which has proven to give an adequate description of molecular LID is the 'strong collision model'. In this model it is assumed that the velocity distribution and the rotational-state distribution reach equilibrium after a single collision, independent of the state before the collision. However, the time scales for

velocity relaxation and rotational relaxation are allowed to differ: see e.g. Mironenko and Shalagin (1981) and Panfilov *et al.* (1983a). An early treatment of the influence of line shape and light intensity was given by Popov *et al.* (1980). A numerical Monte Carlo simulation for several light-induced kinetic effects was given by Kogan *et al.* (1991).

A systematic classification in the spirit of the Chapman–Enskog theory was given by Nienhuis and Van Enk (1991a) using the method of the separation of rapid and slow variables. Both the collision term and the radiative term in the Boltzmann equation are assumed to have an evolution on a time scale which is short compared to the evolution of the flow term. The slow variables—which correspond to quantities that are conserved on the fast time scale—then fully determine the macroscopic state of the gas. The number of these conserved quantities depends on whether a pure gas or a mixture is considered. Their evolution equations take the form of conservation laws. This yields a set of generalized Navier–Stokes equations. Various cases were considered following this approach to elimination of fast variables, see Nienhuis (1989), Van Enk and Nienhuis (1990a, b, 1991a, b), and Nienhuis and Van Enk (1991).

When applying the results of the theory to LIKE in molecular systems, one should bear in mind that they are caused by ro-vibrational excitation. This, of course, has as simplifying feature that the radiative lifetime is long (up to $\approx 1$ s) since the excitation is in the infrared. Since also collisional de-excitation is usually slow compared to the kinetic collision rate, the probability that vibrational de-excitation occurs before the first velocity-changing collision can generally be neglected.



### 3.1. *Light-induced drift; results*

For LID by ro-vibrational excitation of molecules, at least two important differences arise in comparison with the atomic case where the excitation is electronic. First, the rotational sublevels have to be taken into account. Therefore, the elementary two-level model of equation (1) has to be re-examined. However, it was shown by Mironenko and Shalagin (1981) that the existence of rotational substructure within the vibrational states should not dramatically change the formalism as long as the change in collision cross-section $\Delta\sigma/\sigma$ (or in collision rate $\Delta\nu/\nu$) can be considered velocity independent. A similar conclusion was reached by Gel'mukhanov *et al.* (1986b) for the magnetic degeneracy of the sublevels. Therefore equation (1) should still give a reasonable description for molecular LID in the Doppler limit if one were to measure the drift velocity. This brings us to the second important difference compared to atomic LID. Ro-vibrational excitation is found to affect the cross-section for velocity-changing collisions only slightly: typically by 1% or less (for electronic excitation this can be up to 50% (Eliel 1992)). In addition, ro-vibrational excitation addresses only the molecules in a single rotational $(J, K)$ level and therefore limits the fraction of excited molecules $n_e/n_a$ to typically $10^{-3}$. It can now be seen from equation (1) that the drift velocity is limited, typically, to $\sim 10^{-5}$ of the thermal speed. As a consequence, experiments on LID for molecules do not measure $v_{LID}$ directly, but the resulting concentration gradient along a closed tube. A reasonable approximation for the LID-concentration gradient can be easily found from equation (1). In the stationary state the LID flux is compensated by a diffusion flux, i.e.

$$n_a v_{LID} = (n_a + n_b) D \nabla_k x, \tag{10}$$

where $n_b$ is the number density of the buffer gas, $x = n_a/(n_a + n_b)$ the mole fraction of the light-absorbing molecules, $D$ is the diffusion coefficient and the gradient is taken along the propagation vector of the laser light. Upon substitution of equation (1) we find

$$\nabla_k x = -\frac{n_e}{n_a + n_b} \frac{1}{D} \frac{\Delta\sigma}{\sigma} v_L. \tag{11}$$

The value of $n_e$ can be experimentally derived from the absorbed light intensity $I$, by multiplying the number of excitations per unit time and volume with the average time between Maxwellizing collisions, $\tau_e$, for the excited molecules (note that excited molecules whose velocity has been Maxwellized do not contribute to the effect). This yields for a one dimensional system:

$$n_e = -\frac{\nabla_k I}{\hbar\omega} \tau_e. \tag{12}$$

If equation (12) is substituted in the right hand side of equation (11), integration along the length of the cell yields

$$\Delta x = -\frac{\Delta I}{\hbar\omega} \frac{\tau_e}{n_a + n_b} \frac{1}{D} \frac{\Delta\sigma}{\sigma} v_L, \tag{13}$$

for the difference in mole fraction $\Delta x \equiv x_{exit} - x_{entrance}$ between the ends of the closed channel containing the gas mixture under study, with the absorbed light intensity $\Delta I$ taken positive. However, actual experiments are not performed in the idealized case of the Doppler limit. Hence the excitation profile (assumed to be a $\delta$ peak so far) suffers from homogeneous broadening and the velocity selectivity is reduced. Moreover, it turns out to be convenient in the theoretical treatment to consider directly a closed tube with zero net fluxes in the steady state, as shown e.g. by Gel'mukhanov *et al.* (1986a). The more rigorous theoretical result obtained in this way reads (see e.g. Chapovsky *et al.* (1981), Panfilov *et al.* (1983), Gel'mukhanov *et al.* (1986a) or Van der Meer *et al.* (1989)):

$$\Delta n_a = (n_a + n_b)\Delta x = -\frac{2\Delta I}{\hbar\omega v_0} \frac{1}{1 + \nu^a/\nu^b} \frac{\Delta v}{v} \varphi(\Omega), \tag{14}$$

where $v_0 = (2k_B T/m_a)^{1/2}$, the factor $(1 + \nu^a/\nu^b)^{-1}$ containing the frequency of collisions of absorbing molecules with one another ($\nu^a$) and with the buffer gas ($\nu^b$) is a correction factor for experiments outside the limit $n_a \ll n_b$, $\Delta v = v_e^b - v_g^b$, and the 'detuning function' $\varphi(\Omega)$ is given by

$$\varphi(\Omega) = \frac{\int v_x p(v_x)\, dv_x}{v_0 \int p(v_x)\, dv_x}, \tag{15}$$

where $\Omega = \omega_L - \omega_0 = k v_L$ while $n_a p(v_x)\, dv_x$ gives the contribution to the number of excited molecules per unit volume and time due to the particles whose velocity along the $\boldsymbol{k}$ vector lies between $v_x$ and $v_x + dv_x$. Note that for $\delta$ peak excitation one has $p(v_x) \propto \delta(v_x - v_L)$ and $\varphi(\Omega)$ reduces to $v_L/v_0$. The function $\varphi(\Omega)$ obviously depends on the excitation profile $p(v_x)$. It was introduced by Mironenko and Shalagin (1981) and further discussed by Gel'mukhanov *et al.* (1986a). Graphs for various values of the homogeneous linewidth are given by Mironenko and Shalagin (1981) and by Van der Meer *et al.* (1989) for the case that $p(v_x)$ has the shape of a Lorentzian multiplied by a Maxwellian.

It is interesting to notice that the diffusion coefficient does not enter in equation (14). This is a direct consequence of the fact that this formula is derived directly for a closed tube, with the LID mechanism described in terms of friction forces. Equation (14) does reduce to (13) for the Doppler limit with infinite dilution (i.e., $\nu^a/\nu^b \to 0$) upon the identifications

$$\varphi(\Omega) = v_L/v_0,$$

and

$$D = \tfrac{1}{2} v_0^2 \tau,$$

with

$$\frac{\Delta\sigma}{\sigma} \equiv \frac{\Delta\nu}{\nu}.$$

A weak point in the theoretical approaches so far is that $\Delta\nu/\nu$ is considered essentially independent of detuning, i.e., independent of velocity. While this may be a safe approximation for cases in which the buffer particles are light (and therefore essentially determine the relative speed), it is ill-founded in general. This issue has been addressed by Gel'mukhanov *et al.* (1986a). As we will see later on, experiments indicate that great care is in order on this point. Therefore, this question has been quite recently re-examined theoretically by Viehland (1992).



The first pioneering experiments on LID for molecular gases were, just like those for atoms, performed by the Novosibirsk group (Chapovsky *et al.* 1981, Panfilov *et al.* 1981, Panfilov *et al.* 1983a) on $CH_3F$. They employed a steady-state-type technique in a closed tube of $\approx 1$ m long and 1 to 4 mm diameter. Vibrational excitation of the $\nu_3$ fundamental (C–F stretch) was brought about by a $CO_2$ laser ($\lambda \approx 10\,\mu$m). Detection of the concentration difference along the tube was achieved by a mass spectrometer. Measurements were made either in isotropic mixtures or in a buffer gas of He or $H_2$. Values of $\Delta\nu/\nu$ were found to be between $+0{\cdot}4$ and $+1{\cdot}2\%$. Later experiments also investigated the frequency and pressure dependence (Bakarev *et al.* 1986, Chapovsky and Shalagin 1986) and the time dependence of the separation process (Chapovsky and Shalagin 1987). The $CH_3F$ molecule was also studied by Riegler *et al.* (1983).

LID of $^{15}NH_3$ in a $^{14}NH_3$ background was studied by Folin and Chapovsky (1983). Using the 9R(10) line of a $CO_2$ laser, they excited the $\nu_2$ mode of $^{15}NH_3$ which was found to decrease the cross-section by about 5% (as we will see later on, this number may be heavily dependent on the rotational sublevels involved). Later experiments yielded $\Delta\nu/\nu \approx -2{\cdot}5\%$ (Bakarev *et al.* 1988b). Also isotopic mixtures of $CH_3Br$ were studied (Chapovsky 1988) which gave $\Delta\nu/\nu \approx 1\%$. Inverse LID (for which $n_a \gg n_b$) was measured for $CH_3F$ and $CH_3OH$ (Bakarev *et al.* 1988a); the latter molecule was excited into its $\nu_5$ vibrational mode (C–O bond) which was found to produce a value of $\Delta\nu/\nu = 1{\cdot}3\%$.

Also $SF_6$ was studied by this group (Panfilov *et al.* 1983b). Initially, excitation of the $\nu_3$ mode by a $CO_2$ laser was found to produce no measurable effect for a variety of absorption lines and buffer gases. This was attributed to a combination of poor velocity selectivity for this ro-vibrational spectrum and a small value of $\Delta\nu/\nu$ for this antisymmetric vibrational mode. Later experiments yielded a very small positive value: $\Delta\nu/\nu \approx +3 \times 10^{-4}$ in He as buffer gas (Chapovsky 1989).

A different technique was developed by the Leiden group (see Van der Meer *et al.* (1989)). For measuring the concentration difference along a closed tube of 30 cm length and 1 mm radius, a sensitive detection scheme was used based on a differential thermal conductivity measurement (see figure 8). The sensitivity in detecting differences in mole

fraction, $\Delta x$, is $\approx 1$ p.p.m. Measurements were made in real time while the laser was slowly scanned across the absorption profile (see figure 9). The piezo-tunable $CO_2$ laser (tuning range 270 MHz) was given additional tuning capability by using an Acousto Optic Modulator, with a shift of $\pm 90$ MHz for single pass and $\pm 180$ MHz for double pass. Thus a total range of $\approx 600$ MHz could be covered for each line selected by the grating. Alternatively, for studying molecules having absorption bands in the 3 μm region, like $H_2O$ or HF, a continuously tunable colour centre laser was used (Bloemink *et al.* 1992).

From the measured concentration difference $\Delta x$, values of $\Delta v/v$ were derived using equation (14). Experimental data for $\Delta v/v$ resulting from pure vibrational excitation of the $v_3$ fundamental in $CH_3F$ (the isolated Q(12, 3) transition) are given in the table. These data were also used to obtain information on the difference in Lennard-Jones potential parameters between excited and ground-state $CH_3F$, assuming the validity of combination rules (see Section 4).

For ro-vibrational excitation between different rotational sublevels, significant deviations from the standard behaviour (figures 3 and 9) were observed. In some cases, e.g., $C_2H_4$–Kr, the effect can even have either sign depending on the rotational sublevels involved in the same vibrational transition (Van der Meer *et al.* 1992b). This behaviour has been attributed to the dependence of the collision rate $v$ on both the vibrational and the rotational state, with each contribution to $\Delta v/v$ having its own dependence on the relative speed between the collision partners (Chapovsky *et al.* 1992). At the time of writing of this review, this question was still under study.

### 3.2. *Surface light-induced drift; results*

The prediction of SLID dates back to 1983 (Ghiner *et al.* 1983). These authors treated a pure Knudsen gas ($l/R \gg 1$) and used the Maxwell specular/diffuse model.

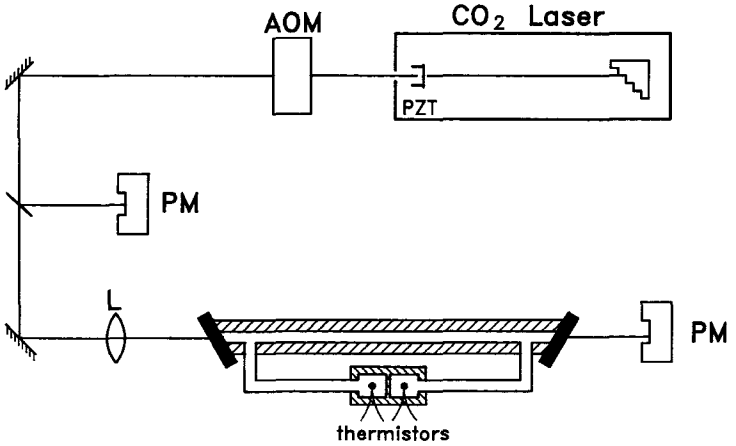


Figure 8. Scheme of the experimental set-up used by Van der Meer *et al.* (1989) for measuring LID in molecular systems. By the combined action of piezo-tuning (PZT) and frequency shift by the acousto–optic modulator (AOM) a total frequency range of 600 MHz is covered for each $CO_2$ laser line. The CW laser has a power of typically 1–3 W. The absorption by the gas mixture, having a pressure of $\sim 133$ Pa $= 1$ Torr, is measured by two power meters (PM). Detection of the concentration difference along the tube (length $L = 300$ mm, radius $R = 1{\cdot}0$ mm) is achieved by two thermistors in the self-heat mode, which act as differential thermal conductivity sensors.

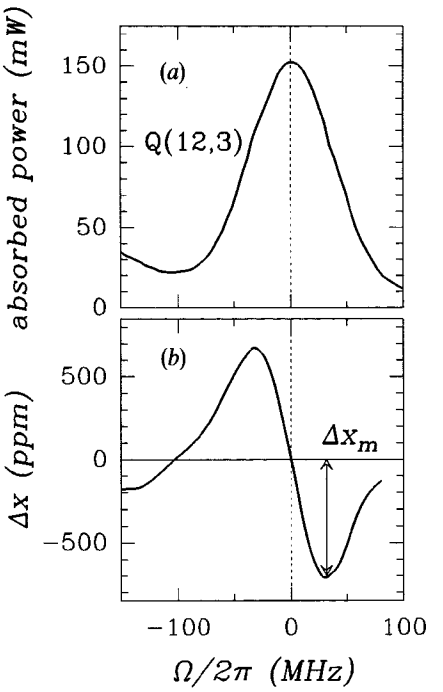


Figure 9. Typical real-time recording of the absorption profile (upper panel) and concentration difference $\Delta x$ (lower panel) in an LID experiment ($x \equiv n_a/(n_a+n_b)$ is the mole fraction of light absorbing particles). The maximum value $\Delta x_m$ is used to derive the change in collision rate upon excitation (see the table). The data pertain to the Q(12, 3) transition within the $\nu_3$ fundamental (C–F stretch) for $CH_3F$; at the left one notices the tail of the Q(12,2) transition. From Van der Meer (1989). (In the original paper, the lower panel actually shows $-\Delta x$).

Experimental values for the relative difference in collision frequency (or in collision cross-section) derived from the maximum of the detected concentration different $\Delta x_m$ in LID measurements as shown in figure 9. The values are for pure vibrational excitation ($\nu_3$-fundamental) of $CH_3F$ colliding with a noble atom; from Van der Meer *et al.* (1989).

| Collision partner | $(\nu_e-\nu_g)/\nu$ $(10^{-3})$ |
|---|---|
| He | $+1{\cdot}4\pm0{\cdot}3$ |
| Ne | $+2{\cdot}5\pm0{\cdot}3$ |
| Ar | $+5{\cdot}5\pm0{\cdot}6$ |
| Kr | $+5{\cdot}6\pm0{\cdot}4$ |
| Xe | $+5{\cdot}6\pm0{\cdot}5$ |

Later treatments also considered the case of higher densities, with $l/R \ll 1$ (Ghiner and Vaksman 1984, Vaksman and Ghiner 1985, Roldugin 1988, Van Enk and Nienhuis 1991b). In connection with the experimental results for this effect, Hoogeveen *et al.* (1990a) treated SLID for the Knudsen limit case along the lines of the theory established for LID. They assumed a two-level model, which is justified by the fact that, in the absence of intermolecular collisions, the excited molecular cannot change its

internal quantum numbers before colliding with the surface. The magnitude of the drift velocity was found to be

$$v_{\mathrm{SLID}} = -\frac{\alpha_e - \alpha_g}{\alpha_g}\frac{n_e}{n} v_0 \varphi(\Omega), \tag{16}$$

where $\alpha_i$ is the accommodation coefficient for tangential momentum in state $i$; this is the average fraction of the tangential momentum that a molecule transfers to the surface in a single collision. The expression (16) is in perfect analogy with the case of LID if $\Delta\alpha/\alpha$ is replaced by $\Delta\sigma/\sigma$, and reduces to (5) for $\delta$-peak excitation. Observation of SLID is achieved by monitoring the resulting pressure difference between the ends of a closed channel (Hoogeveen *et al.* 1987). This pressure difference, $\delta p$, is easily derived from equation (16) in the steady-state, where the light-induced flux is balanced by a Knudsen flow driven by $\delta p$. Using the expression for a Knudsen particle flow through a round channel of radius $R$ and length $L$ (Kennard 1938)

$$\Phi = \frac{2\pi}{3} R^3 \frac{\bar{v}}{kT}\frac{2-\alpha}{\alpha}\frac{\delta p}{L}, \tag{17}$$

with $\bar{v} = (8kT/\pi m)^{1/2}$, one finds using $\pi R^2 n v_{\mathrm{SLID}} = \Phi$:

$$\frac{\delta p}{p} = -\frac{3\sqrt{\pi}}{4}\frac{L}{R}\frac{n_e}{n}\frac{\Delta\alpha}{2-\alpha}\varphi(\Omega), \tag{18}$$

where $\Delta\alpha \equiv \alpha_e - \alpha_g$.

If $\alpha$ is close to unity (which is usually the case) a further simplification can be made, i.e., $\Delta\alpha/(2-\alpha) \approx \Delta\alpha$. Note that the appearance of the geometry factor $L/R$ in equation (18) can increase the sensitivity of these measurements by a few orders of magnitude.

In the Knudsen limit with $\alpha$ near unity, $n_e$ can be related to the observed absorption in a particularly easy way. Since the radiative lifetime is long for vibrational excitation, the total number of excitations in the tube per unit time, $\pi R^2 \Delta I/\hbar\omega$, equals the number of excited molecules colliding with the surface per unit time, $\frac{1}{4} n_e \bar{v} 2\pi RL$. This yields

$$n_e = \frac{\Delta I}{\hbar\omega L}\frac{2R}{\bar{v}}. \tag{19}$$

This result can also be looked upon as the number of excitations per unit volume and time, multiplied by the average time between successive molecule-wall collisions.

It is interesting to note that a good approximation to equation (18) can be directly obtained from elementary considerations in the Doppler limit where $\varphi(\Omega) = v_L/v_0$ (Hoogeveen *et al.* 1987). In the stationary state the net force on the gas vanishes. Hence the net tangential momentum delivered to the tube wall per second which can be approximated by $2\pi RL\frac{1}{4} n_e \bar{v} m v_L \Delta\alpha$, is compensated by the net force $\pi R^2 \delta p$ on the end faces. After some trivial manipulation this yields equation (18) with a slightly different numerical factor. This difference (a factor $3\pi/8$) is caused by the fact that the excited particle flux on the tube wall has been approximated by its equilibrium value $\frac{1}{4} n_e \bar{v}$.

The first experimental observation of SLID was given by Hoogeveen *et al.* (1987). These experiments were performed in low pressure $CH_3F$ ($0{\cdot}5\,\mathrm{Pa} \leqslant p \leqslant 20\,\mathrm{Pa}$), ro-vibrationally excited into the $\nu_3$ mode. The gas was contained in a quartz capillary having length $L = 300\,\mathrm{mm}$ and radius $R = 0{\cdot}75\,\mathrm{mm}$, thus yielding a geometry factor of $L/R = 400$ (see equation (18)). The set-up was essentially identical to that used for LID (figure 8) with the concentration detection replaced by a sensitive differential

capacitance manometer. Real-time recordings of such experiments are shown in figure 10. The maximum values of the observed relative pressure difference, $\delta p_m/p$, normalized by the excited state fraction is then displayed as a function of $p$. An example of such a graph is shown in figure 11 for the R(4, 3) transition, i.e., $(v, J, K) = (0, 4, 3) \rightarrow (1, 5, 3)$. From the low pressure value, which should be independent of pressure according to equation (18), the value of $\Delta\alpha \equiv \alpha_e - \alpha_g$ is determined.

Somewhat surprisingly, experiments on this $v = 0 \rightarrow 1$ vibrational transition involving different $(J, K)$ levels showed that the accommodation coefficient is much more sensitive to changes in the rotational than in the vibrational state (Hoogeveen *et al.* 1987): For the Q(12, 2) transition (which has $\Delta J, \Delta K = 0$) no effect was detected, while for the R(4, 3) transition ($\Delta J = 1$, $\Delta K = 0$) the value of $\Delta\alpha$ was found to be positive: $\Delta\alpha = 1{\cdot}9 \times 10^{-3}$ for $CH_3F$–quartz (Hoogeveen *et al.* 1990a).

Further experiments on $CH_3F$ and OCS (Broers *et al.* 1991, Van der Meer *et al.* 1992a) confirmed that $\alpha$ increases with increasing $J$ for small values of $J$, i.e., $J \ll J_{\text{thermal}}$.

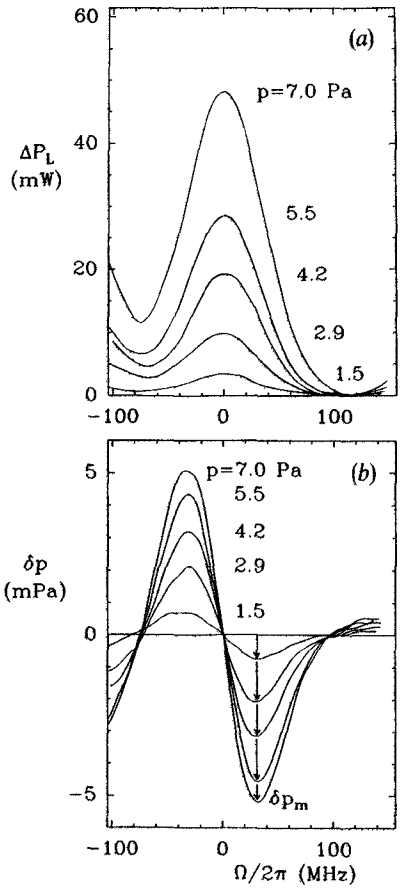


Figure 10. Direct real-time measurements of absorption (upper panel) and pressure difference (lower panel) in a typical SLID experiment. The data pertain to the R(4, 3) transition of the $\nu_3$ fundamental (C–F stretch) in $CH_3F$, with the tail of the neighbouring R(4, 2) line showing up at the left. The value of $\delta p_m$ in the Knudsen limit is used to determine the change in accommodation coefficient for tangential momentum upon excitation (see figure 11 and equation (18)). From Hoogeveen *et al.* (1990a).

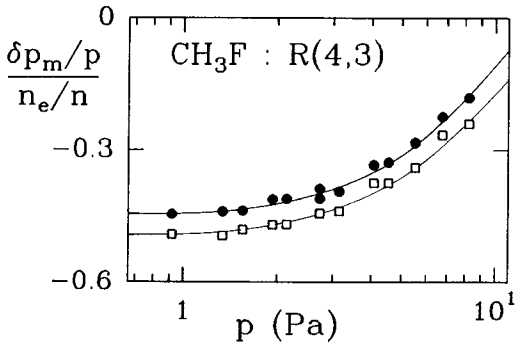


Figure 11. Values of the normalized maximum pressure difference measured in an SLID experiment (see figure 10). From the low-pressure limit the value of $\Delta\alpha$ is found using equation (18). The data show that $\alpha$ increases for $CH_3F$ upon the transition $J=4\rightarrow5$, $K=3\rightarrow3$. These data pertain to a flat channel with the linear light polarization parallel (●) or perpendicular (□) to the surface. They show that the accommodation increase is larger if the molecule rotates with $\boldsymbol{J}\parallel$ surface ('cartwheel') that with $\boldsymbol{J}\perp$ surface ('helicopter'). Data from Broers *et al.* (1991).



For $J \gg J_{\text{thermal}}$ the opposite was found in molecular-beam-type experiments, e.g. by Mödl *et al.* (1985) for NO–Ge. This seemingly contradictory result was reconciled in the unified kinetic description developed by Borman *et al.* (1988) extended to rotating molecules (Hoogeveen *et al.* 1990b, Borman *et al.* 1991), where $\alpha$ was found to peak near $J_{\text{thermal}}$.

Results on SLID for OCS and for $CH_3F$ with various surfaces and surface conditions were given by Van der Meer *et al.* (1992a). It was found that all cases studied were in qualitative agreement with the unified kinetic description mentioned above. Quantitatively, the effects for a LiF(100) surface were found to be an order of magnitude larger than those measured e.g. for a quartz surface which must be assumed to be covered by adsorbates at the experimental conditions.

Another interesting feature revealed by SLID experiments is the dependence of molecule–surface interaction upon the angle between the rotational axis of the molecule and the surface. This was studied by using a flat channel and linearly polarized light, with the axis of polarization either parallel or perpendicular to the surface (Broers *et al.* 1991) (see figure 11). It was found that, for low $J$, molecules having $\boldsymbol{J}$ parallel to the surface (the 'cartwheel mode') have a higher accommodation than those having $\boldsymbol{J}$ perpendicular ('helicopter mode'). For high $J$ the opposite was found, which is in agreement with desorption experiments by Jacobs *et al.* (1987). This behaviour was attributed to the role of rotational (de)-excitation in molecule–surface collisions (Broers *et al.* 1991).

### 3.3. *Light-induced pressure anisotropy and light-induced heat flux; results*

As mentioned in Section 2, momentum conservation requires that, in a pure gas, the first moment of the velocity distribution vanishes, i.e., LID cannot occur. This does not exclude kinetic effects from higher moments to occur. This was first pointed out by Levin and Folin (1980) for the light-induced heat flux (i.e., non-vanishing third moment), and subsequently by Folin *et al.* (1981) for heat flux and pressure anisotropy (i.e., change in second moment). Expressions were given for δ-peak excitation: see equations (6) and (7). More general cases, including the case of inhomogeneous light

intensity, were treated by Ghiner (1982) and by Ghiner *et al.* (1982), who also obtained an explicit form of the velocity distribution.

These effects emerge in a natural way in the general formalism by Nienhuis (1989) based on the method of elimination of rapid variables. The zeroth order in the expansion parameter $\varepsilon(\propto Kn = l/R)$ yields the main contributions already given in equations (6) and (7). These are linear in the light intensity. The first-order solution yields contributions with a different detuning behaviour, given in figure 2 in the paper by Nienhuis (1989). These are linear in the intensity gradient, and smaller than the zeroth-order contributions by typically a factor $l/R$. An extension to broadband excitation was given by Van Enk and Nienhuis (1990a). The case of binary mixtures was treated also by these authors (Van Enk and Nienhuis 1992b). In this case an additional effect arises if the light intensity is inhomogeneous, i.e. diffusive pulling. This effect was treated earlier by Gel'mukhanov and Shalagin (1979b) (see Eliel (1992) for experimental data). It arises due the fact that, if the cross-section increases upon excitation, the diffusion coefficient in high-intensity regions is smaller than in low-intensity regions. This causes a density gradient in the direction of the light intensity gradient. Note that this effect occurs also if the excitation is not velocity-selective.

Experimentally, light-induced pressure anisotropy should be easily observable in principle: as follows from equation (6), for typical values of $\Delta\sigma/\sigma = 1 \times 10^{-2}$ and $n_e/n = 1 \times 10^{-3}$ one finds $\delta p/p = 1 \times 10^{-5}$ at exact resonance ($v_L = 0$). This is more than one order of magnitude larger than the detection limit at $p \approx 100$ Pa. In practice, measurements of the pressure anisotropy is not trivial if the absorption is small, since any tubing connecting the illuminated gas with the differential manometer monitors $p_{yy}(=p_{zz})$. Therefore, strong absorption is needed, either by the gas or by the cell wall, such that the gas near the exit of the tube is in the dark. In the stationary state, its (isotropic) pressure is then determined by $p_{xx}$ in the illuminated part. However, attempts to measure $\delta p$ were unconvincing so far (Hoogeveen *et al.* 1986), since $\delta p$ was found to be overwhelmed by the larger pressure effects arising from non-uniform illumination (see Section 2.4 and 3.4).

Experimental verification of light-induced heat flux may be performed by measuring the temperature difference between the ends of a cell with thermally isolating walls. However, in such an experiment one has to realize that velocity-selective excitation will inevitably be accompanied by a flux of excitation energy which has a first-moment character. For molecules, the ro-vibrational excitation energy is transformed into heat (by molecule–molecule and molecule–surface collisions), thereby heavily interfering with the LIHF effect. An estimate of the ratio of third to first moment heat flux can be easily derived since in the first moment heat flux all the excitation energy, $h\nu_L$, is transported, whereas in the third moment heat flux only a small fraction $\Delta\sigma/\sigma$ of the kinetic energy $k_B T$ is transported. This results in a ratio $(\Delta\sigma/\sigma)k_B T/h\nu_L$. With typical values $\Delta\sigma/\sigma = 1 \times 10^{-2}$, $k_B T/h\nu_L = 0{\cdot}2$, one arrives at a ratio of $2 \times 10^{-3}$. This shows that measurement of the third moment heat flux is practically impossible. A similar conclusion was reached by Chapovsky and Shalagin (1985).

### 3.4. *Light-induced viscous flow; results*

It was noticed already by Levin and Folin (1980) that an intensity gradient perpendicular to the wave-vector produces stresses in a light-absorbing gas if the collision cross-section is state dependent. This is compensated by a velocity gradient, such that the total stress vanishes in the stationary state for an open tube. However,

these authors—who called this effect photo-induced viscosity—did not include momentum exchange with the boundary. Hence the result of their treatment is a circulation pattern in the gas with the total momentum remaining zero. Essentially the same result was obtained by Ghiner (1982) and by Ghiner *et al.* (1982), who assumed specular reflection in molecule-wall collisions.

If the velocity field produced by the above stresses is anchored to the wall by a non-zero accommodation coefficient for tangential momentum, a net flow through the cross-section of the channel will occur. This case was treated by Hoogeveen *et al.* (1989a) along the lines of the Chapman–Enskog theory for the near-hydrodynamic limit ($l \ll R$) in a round tube. Under these conditions the flow velocity at the wall can be assumed to vanish: $v(R)=0$ (stick boundary condition). The resulting velocity profile was found to be given by

$$v_{\mathrm{LIVF}}(r)=\frac{\pi}{2} v_{\mathrm{L}} \frac{\Delta v}{v}\left[\frac{n_{\mathrm{e}}(r)}{n}-\frac{n_{\mathrm{e}}(R)}{n}\right], \tag{20}$$

where the $r$ dependence of the excited-state fraction $n_e/n$ reflects the gradient in the light intensity $I$. For weak absorption, $n_e \propto I$ and the velocity profile follows the intensity profile minus its value at the boundary (see figure 12(*a*, *b*)).

In a closed tube a pressure difference $\delta p$ between the ends of the tube arises, and in the stationary state the light-induced flow integrated over the cross-section of the tube is compensated by a Poiseuille back flow (see figure 12(*c*)). It may seem that further

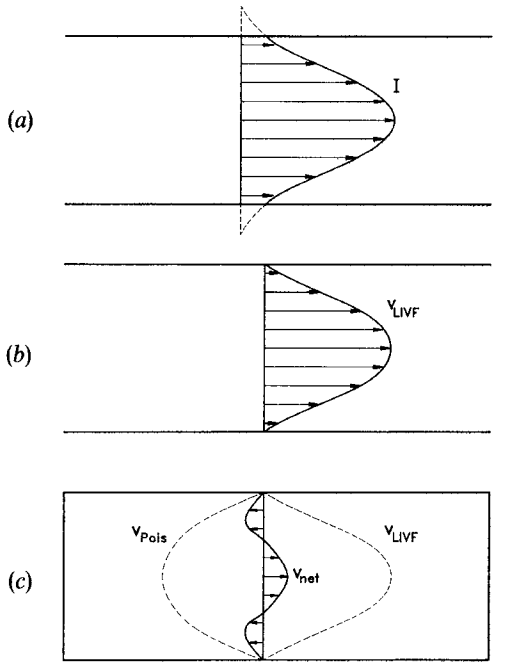


Figure 12. Schematic picture of intensity and flow profiles in LIVF. (*a*) Light-intensity profile, assumed to be Gaussian with non-vanishing intensity at the wall of the tube: $I(R)\neq 0$. (*b*) Resulting flow profile through an open tube (see equation (20)) with stick-boundary-condition: $v(R)=0$. (*c*) Flow profile in a closed tube: the LIVF profile is compensated by a Poiseuille back flow such that the net flow over the tube cross-section vanishes.

evaluation requires knowledge about the exact form of $n_e(r)$ and thus of the intensity profile. However, if one assumes $n_e(R)=0$, it follows from equation (20) that $v_{LIVF}(r) \propto n_e(r)$. By integrating both quantities over the cross-section of the tube, one finds that the total flow (and thus $\delta p$) is proportional to the integrated light intensity (and thus to the absorbed laser power), irrespective of the shape of the light intensity profile. Hence one arrives at

$$\left(\frac{\delta p}{p}\right)_{LIVF} = 16 \frac{L}{R} \frac{l}{R} \frac{v_L}{\bar{v}} \frac{\Delta v}{v} \frac{\bar{n}_e}{n}, \tag{21}$$

where $\bar{n}_e$ is the tube-averaged excited-state density derived from the absorption (Hoogeveen *et al.* 1989a).

An independent treatment leading to essentially the same result was given by Van Enk and Nienhuis (1991b) in the framework of the method of elimination of fast variables.

Experimental investigation of this effect (which, in fact, preceded the theoretical interpretation) by Hoogeveen *et al.* (1989a) was achieved in the set-up similar to that employed for SLID, except that the (one-component) gas must be at sufficiently high density to have $l \ll R$. With $R=0{\cdot}75$ mm this requires $p \gg 5$ Pa. An upper limit is imposed by pressure broadening and by the $p^{-1}$ decay of the effect (see equation (21)). This reduces the effective pressure range to $30\,\text{Pa} \leqslant p \leqslant 150\,\text{Pa}$.

In order to rule out a substantial contribution from SLID at these pressures, this effect was studied for the Q(12,2) and Q(12,3) transition in $CH_3F$; these purely vibrational transitions, having $\Delta J$, $\Delta K=0$, were found to produce a negligible SLID contribution (see Section 3.2). This choice also ensures that inelastic contributions can

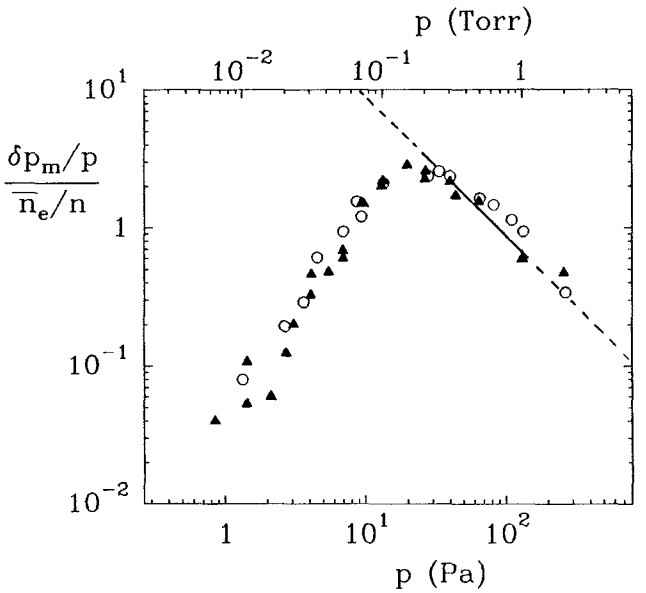


Figure 13. Experiment and theory for light-induced viscous flow. The data points are for $CH_3F$. They give the maximum of the observed pressure difference for positive detuning, normalized by the excited-state fraction, as a function of pressure for the Q(12, 2) transition (triangles) and the Q(12, 3) transition (circles). The solid line gives the theoretical result, equation (21), for the near-hydrodynamic limit. From Hoogeveen *et al.* (1989a).

be disregarded (see Section 3.5). Consequently, the theoretical model developed for this phenomenon should apply, and equation (21) should give a good description of the experiment. Indeed, as seen in figure 13, the data are found to be well described by equation (21) in the effective pressure range mentioned above. Note that this description contains no adjustable parameters, since $\Delta v/v$ for pure $CH_3F$ is known from LID experiments in isotopic mixtures: $\Delta v/v = 1{\cdot}1 \times 10^{-2}$ for the Q(12, 2) and Q(12, 3) transitions (Panfilov *et al.* 1983a).

### 3.5. *Velocity-selective heating; results*

As pointed out in Section 2.5, velocity selective optical excitation immediately followed by collisional de-excitation gives rise to 'velocity-selective heating'. This creates an anisotropy in the temperature and hence also in the transport coefficients. Therefore, this phenomenon can in principle be measured in terms of a heat flux, a momentum flux or—in mixtures—as a diffusive flux.

Heat flux measurements do not seem easily feasible: for the reasons discussed in Section 3.3 it is difficult to distinguish the contribution under study from other—larger—effects.

The case of diffusion seems more attractive. Indeed, the mechanism of velocity-selective heating may give huge contributions to LID if the de-excitation energy is large. However, as discussed by De Lignie and Woerdman (1990) this requires that the scattering process associated with the de-excitation be anisotropic (forward or backward preference). Without detailed knowledge about the collision dynamics, no clear-cut demonstration of this mechanism is therefore possible from LID experiments.

The case of momentum transport in a pure gas offers a better perspective. Here the transported quantity is not the particles themselves but their momentum, and momentum conservation eases the treatment (see figure 6). For this case, an elementary treatment was given by Hoogeveen and Hermans (1991) to explain light-induced viscous flow driven by this mechanism. A perfect analogy with the 'elastic' LIVF case was found, provided that $\Delta v/v$ for the elastic case (equation (21)) was replaced by $-\Delta\eta/\eta$ resulting from the heating–cooling mechanism (see equation (9)). This seems reasonable since $\eta \propto \sigma^{-1} \propto v^{-1}$. One thus has for the pressure difference resulting from this mechanism:

$$\left(\frac{\delta p}{p}\right)_{\Delta T} = -16\,\frac{L}{R}\,\frac{l}{R}\,\frac{v_L}{\bar{v}}\,\frac{\bar{n}_e}{n}\,\frac{1}{\eta}\,\frac{\mathrm{d}\eta}{\mathrm{d}T}\,\frac{f\Delta E_{rot}}{3k_B}. \tag{22}$$

This phenomenon was also treated by Van Enk and Nienhuis (1991a) using the method of elimination of fast variables. In this case, slow variables are defined by requiring that they are *nearly* conserved during the rapid processes, such that they vary only on the slow time scale. The point is, that laser excitation and subsequent collisional de-excitation affects only a small group of molecules, so that conservation of translational energy is only slightly violated. Their result for the pressure difference due to the combination of LIVF and velocity-selective heating is given in the form

$$\frac{\delta p}{p} = -16\,\frac{L}{R}\,\frac{\eta^2 \bar{U} v_L}{p^2 n R}\left(\frac{\Delta E_{rot}}{6kT}\,\frac{2f}{1+f} - \frac{\Delta v}{v}\right), \tag{23}$$

where

$$\bar{U} = \frac{\Delta L}{\hbar\omega L},$$

is the average number of photons absorbed per unit of time and volume. The main difference between this result and the expressions (21) and (22) is the replacement of

$$\frac{\Delta E_{\text{rot}}}{kT},$$

in equation (23) by

$$\frac{2}{\eta}\frac{\partial \eta}{\partial T}\frac{\Delta E_{\text{rot}}}{k},$$

in equation (22), which is equivalent for a hard sphere model.

A quite different way to look at this phenomenon was put forward by Hess and Hermans (1992). They pointed out that the observed pressure difference can be looked upon as Maxwell's thermal pressure resulting from the inhomogeneous heat flux inherent to the phenomenon of velocity-selective heating–cooling in a spatially inhomogeneous intensity profile. In this case, the heat flux is not brought about by an applied temperature gradient. This makes this concept ideal to verify the existence of Maxwell's thermal pressure, which is difficult to observe in the traditional way.

Experimentally, a convenient case to study is $CO_2$ at elevated temperature. For hot-band ro-vibrational excitation by a $CO_2$ laser, all transitions are coincident with the laser lines. In addition, R and P lines can be employed such that both velocity-selective heating and cooling can be achieved (the vibrational part of the excitation can be disregarded here since de-excitation is several orders of magnitude slower, giving rise to isotropic heating only). Experimental results for this case were first obtained by Hoogeveen and Hermans (1990) and are shown in figure 14. Similar data were obtained also for $CH_3F$, $CD_3F$ and $C_2H_4$ (Hoogeveen and Hermans 1991).

The experimental results can also be expressed in terms of the underlying change in viscosity, $\Delta\eta/\eta$. This is shown on the right in figure 14. If these values are compared with those calculated on the basis of the rotational energy $\Delta E_{\text{rot}}$ (see equation (9)) one finds an experimental value for $f$. For $CO_2$ and $CH_3F$, where the vibration can be disregarded, the result was found to compare favourably with the ratio of the rotationally inelastic to the elastic cross-section. This agreement—and the linear behaviour in figure 14—seems to confirm the validity of the given description.

An interesting point is that the effect due to velocity-selective heating/cooling is seen to be an order of magnitude larger than the effect due to a mere change in cross-section. The latter is found directly from the value at the intercept, where $\Delta E_{\text{rot}} = 0$. This makes the present mechanism a potential handle to generate large light-induced kinetic effects for molecules for which the mechanism relying on a change in cross-section is ineffective.

## 4. Applications of light-induced kinetic effects

The field of LIKE, in addition to producing interesting and conceptually new gas-kinetic phenomena, has seen various applications. Some of these have already been mentioned. Let us first recall that LID and SLID provide an inherently differential (and therefore sensitive) tool to obtain information on internal-state-dependent molecule–molecule and molecule–surface interaction, respectively. In the former case, LID data for $CH_3F$-noble gases were used to determine model potential parameters for the vibrationally excited $CH_3F$ potential (Rautian *et al.* 1983, Hoogeveen *et al.* 1989b). In the latter, SLID measurements have provided state-specific information on the role of

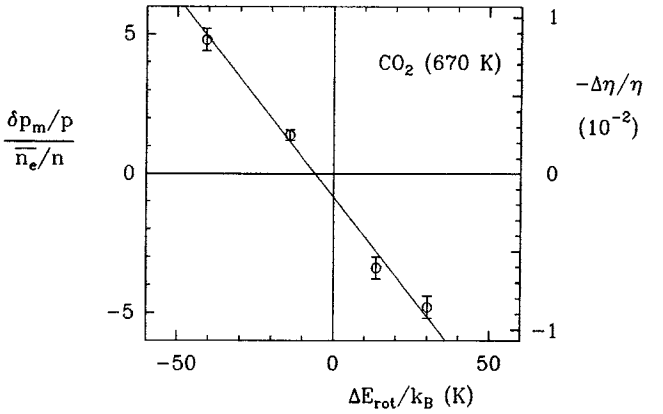


Figure 14. The effect of velocity-selective heating/cooling demonstrated for the case of momentum transport (see figure 7). Displayed is the maximum of the observed pressure difference for positive detuning, normalized by the average excited state fraction, as a function of the rotational part of the excitation energy. The right-hand scale gives the corresponding values of $-\Delta\eta/\eta$ derived from the data using equation (22). The data points correspond to the transitions (left to right): P(32), P(12), R(12) and R(32) in the 9 μm band. From Hoogeveen and Hermans (1990).



the rotational state in molecule–surface collisions. This includes both the magnitude of the rotational quantum numbers ($J$, $K$) (Hoogeveen *et al.* 1990a) and the direction of $\boldsymbol{J}$ with respect to the surface normal (Broers *et al.* 1991). The applicability of this information was extended to all coefficients characterizing molecule surface accommodation, including the trapping probability, by the unified kinetic approach developed by Borman *et al.* (1988).

Another application of LIKE is isotope separation by LID. This has been achieved in the molecular case for $^{12}CH_3F$–$^{13}CH_3F$ mixtures (Chapovsky *et al.* 1981) and for $^{14}NH_3$–$^{15}NH_3$ mixtures (Folin and Chapovsky 1983), and in the atomic case for rubidium atoms in a noble gas background (see Eliel (1992)).

LID was also used to study nuclear spin conversion rates for the ortho and para modifications of $CH_3F$ (Chapovsky *et al.* 1985, Bakarev and Chapovsky 1986, Chapovsky 1991). It was found, quite surprisingly, that the conversion times are $\approx 1$ h for $^{12}CH_3F$ and only 1·2 min for $^{13}CH_3F$.

Another interesting idea for an application of LID is due to Kogan *et al.* (1990) who proposed to use LID to spatially separate reaction products in a photochemical reaction.

A method to use LID for increasing the sensitivity in detecting traces of a light-absorbing species in a background gas was suggested by Atutov *et al.* (1991). For Na in a Xe background, an increase in sensitivity by a factor $2 \times 10^3$ was demonstrated.

Possible applications of LID in the field of astrophysics have been mentioned by Atutov and Shalagin (1987, 1988). Noting that this mechanism can be much stronger than radiation pressure, they suggested that it could be the cause of the anomalous isotope distributions observed in some stars. The possible mechanisms that could lead to velocity-selective excitation in astrophysical situations have also been reviewed by Eliel (1992). An interesting case intimately related to the molecular systems discussed in the present paper is the possible role of LID in explaining the peculiar behaviour of the deuterium abundance relative to hydrogen for the various planets in our solar system.

The D/H ratio, being $1{\cdot}5 \times 10^{-4}$ on our planet, is two orders of magnitude larger on Venus, whereas for the outer planets it approaches the cosmic value of $\approx 10^{-5}$. Traditional explanations have remained unsatisfactory (Grinspoon 1987). As noted by Atutov and Shalagin (1987, 1988), LID for $H_2O$ during the early stages of the solar system may have been an effective mechanism: it combines the great isotope-selectivity inherent to spectral lines with a means to physically displace particles. In their model, the protosun would have acted as the radiation source, causing ro-vibrational excitation of $H_2O$ in the colder-outer regions. The necessary velocity selectivity would have been provided by gravitational redshift. This scheme would push $H_2O$ preferentially outward, thus increasing the D/H ratio near the centre provided that the value of $\Delta\sigma/\sigma$ (equation (1)) is positive and not too small. Experiments to investigate the feasibility of this idea have been performed by Bloemink *et al.* (1992).

## 5. Conclusions

The combination of velocity-selective excitation and state-dependent interaction provides a new and direct way to manipulate the velocity-distribution of a gas without imposing external gradients. For molecules in a buffer gas background (or at such low pressure that molecule–surface collisions are important) a drift of the gas can occur. In a pure gas, where momentum conservation precludes such a drift, other effects corresponding to higher moments of the velocity distribution can arise. In addition, a gradient of the light intensity can produce stresses in the gas, which translate into a net flow if momentum exchange with the surrounding vessel is taken into account.

A special type of light-induced kinetic effect occurs when velocity-selective excitation is followed by rapid collisional de-excitation. A manifestation of such 'velocity-selective heating/cooling' is demonstrated for the case of a viscous flow in an inhomogeneous laser field.

Most experimental results are well-described by the theoretical models assuming a velocity-independent change in collision rate upon excitation. The experiments on light-induced drift through a buffer gas yield information on the internal-state dependence of the intermolecular potential. Data on surface light-induced drift have been used to obtain information on rotational-state-dependent molecule–surface interactions. The data are in agreement with the unified kinetic approach by Borman *et al.*, suggesting that the various accommodation coefficients—including the trapping probability—as a function of the rotational quantum number $J$ peak around the thermal value of $J$. In addition, interesting information has been obtained on the role of the alignment of the rotational axis with respect to the surface ('helicopter' versus 'cartwheel' rotation).

Further applications include isotope separation, studies of ortho–para conversion and possible astrophysical applications.

## Acknowledgments

The author is pleased to acknowledge critical comments by P. L. Chapovsky, J. J. M. Beenakker, H. I. Bloemink, E. R. Eliel, S. J. van Enk, G. J. van der Meer and G. Nienhuis.

This work is part of the research programme of the Foundation for Fundamental Research on Matter (FOM) and was made possible by financial support from The Netherlands Organization for Scientific Research (NWO).

## References


ANTSYGIN, V. D., ATUTOV, S. N., GEL'MUKHANOV, F. KH., TELEGIN, G. G., and SHALAGIN, A. M., 1979, *Pis'ma Zh. eksp. teor. Fiz.*, **30,** 262 (*JETP Lett.*, **30,** 243).

ATUTOV, S. N., and SHALAGIN, A. M., 1987, *Preprint*, 370*a*, Institute of Automation and Electrometry, Novosibirsk; 1988, *Soviet Astron. Lett.*, **14,** 284 (*Pis'ma Astron. Zh.*, **14,** 664).

ATUTOV, S. N., POD'YACHEV, S. P., and SHALAGIN, A. M., 1991, *Optics Commun.*, **83,** 307.

BAKAREV, A. E., and CHAPOVSKY, P. L., 1986, *Pis'ma Zh. eksp. teor. Fiz.*, **44,** 5 (*JETP Lett.*, **44,** 4).

BAKAREV, A. E., FOLIN, A. K., and CHAPOVSKY, P. L., 1988b, *Zh. eksp. teor. Fiz.*, **94,** 66 (*Soviet Phys. JETP*, **67,** 903).

BAKAREV, A. E., ISHIKAEV, S. M., and CHAPOVSKY, P. L., 1988a, *Kvantovaya Elektronika*, **15,** 1418 (*Soviet J. Quantum Electron.*, **18,** 890).

BAKAREV, A. E., MAKAS, A. L., and CHAPOVSKY, P. L., 1986, *Soviet J. quant. Electron.*, **16,** 16.

BERMAN, P. R., HAVERKORT, J. E. M., and WOERDMAN, J. P., 1986, *Phys. Rev.* A, **34,** 4647.

BLOEMINK, H. I., BOON-ENGERING, J. M., ELIEL, E. R., and HERMANS, L. J. F., 1992 (to be published).

BORMAN, V. D., KRYLOV, S. YU., HERMANS, L. J. F., and PANKOV, A. YU., 1991, *Proceedings of the 17th International Symposium on Rarefield Gas Dynamics*, edited by A. E. Beylich (New York: Weinheim), p. 1435.

BORMAN, V. D., KRYLOV, S. YU., and PROSYANOV, A. V., 1988, *Zh. eksp. teor. Fiz.*, **94,** 271 (*Soviet Phys. JETP*, **67,** 2110).

BROERS, B., VAN DER MEER, G. J., HOOGEVEEN, R. W. M., and HERMANS, L. J. F., 1991, *J. chem. Phys.*, **95,** 648.

CHAPOVSKY, P. L., 1988, *Kvantovaya Elektronika*, **15,** 738; 1989, *Izvestiya Akad. Nauk. SSSR, Ser. Fiz.*, **53,** 1075 (*Bull. Acad. Sci. USSR, Phys. Ser.*, **53,** 43); 1991, *Phys. Rev.* A, **43,** 3624.

CHAPOVSKY, P. L., KRASNOPEROV, L. N., PANFILOV, V. N., and STRUNIN, V. P., 1985, *Chem. Phys.*, **97,** 449.

CHAPOVSKY, P. L., and SHALAGIN, A. M., 1985, *Soviet J. quant. Electron.*, **15,** 1500; 1986, *Ibid.*, **16,** 1649; 1987, *Ibid.*, **17,** 355.

CHAPOVSKY, P. L., SHALAGIN, A. M., PANFILOV, V. N., and STRUNIN, V. P., 1981, *Optics Commun.*, **40,** 129.

CHAPOVSKY, P. L., VAN DER MEER, G. J., SMEETS, J., and HERMANS, L. J. F., 1992, *Phys. Rev.* A, (in press).

DYKHNE, A. M., and STAROSTIN, A. N., 1980, *Zh. eksp. teor. Fiz.*, **79,** 1211 (*Soviet Phys. JETP*, **52,** 612).

ELIEL, E. R., 1992, *Adv. atom. molec. and opt. Phys.*

VAN ENK, S. J., and NIENHUIS, G., 1990a, *Phys. Rev.* A, **41,** 3757; 1990b, *Ibid.*, **42,** 3079; 1991a, *Ibid.*, **44,** 7615, 1991 b, *Physica* A, **179,** 199.

FOLIN, K. G., and KOMAROV, K. P., 1980, *Optics Commun.*, **35,** 351.

FOLIN, A. K., FOLIN, K. G., GHINER, A. V., and KOMAROV, K. P., 1981, *Optics Commun.*, **36,** 462.

FOLIN, A. K., and CHAPOVSKY, P. L., 1983, *Pis'ma Zh. eksp. teor. Fiz.*, **38,** 452 (*JETP Lett.*, **38,** 549).

GEL'MUKHANOV, F. KH., 1984a, *Soviet Phys. Dokl.*, **29,** 45; 1984b, *Soviet J. quant. Electron.*, **14,** 347.

GEL'MUKHANOV, F. KH., and IL'ICHOV, L. V., 1983, *Chem. Phys. Lett.*, **98,** 349; 1985a, *Zh. eksp. teor. Fiz.*, **88,** 40; 1985b, *Optics Commun.*, **53,** 381.

GEL'MUKHANOV, F. KH., IL'ICHOV, L. V., and SHALAGIN, A. M., 1986a, *Physica* A, **137,** 502; 1986b, *J. Phys.* A, **19,** 2201.

GEL'MUKHANOV, F. KH., and SHALAGIN, A. M., 1979a, *Pis'ma Zh. eksp. teor. Fiz.*, **29,** 773 (*JETP Lett.*, **29,** 711); 1979b, *Zh. eksp. teor. Fiz.*, **77,** 461 (*Soviet Phys. JETP*, **50,** 234).

GHINER, A. V., 1982, *Optics Commun.*, **41,** 27.

GHINER, A. V., KOMAROV, K. P., and FOLIN, K. G., 1982, *Zh. eksp. teor. Fiz.*, **82,** 1853 (*Soviet Phys. JETP*, **55,** 1068).

GHINER, A. V., STOCKMANN, M. I., and VAKSMAN, M. A., 1983, *Phys. Lett.* A, **96,** 79.

GHINER, A. V., and VAKSMAN, M. A., 1984, *Phys. Lett.* A, **100,** 428.

GRINSPOON, D. H., 1987, *Science*, **238,** 1702.

HESS, S., and HERMANS, L. J. F., 1992, *Phys. Rev.* A, **45,** 829.

HOOGEVEEN, R. W. M., and HERMANS, L. J. F., 1990, *Phys. Rev. Lett.*, **65,** 1563; 1991, *Phys. Rev.* A, **43,** 6135.

HOOGEVEEN, R. W. M., HERMANS, L. J. F., BORMAN, V. D., and KRYLOV, S. YU., 1990b, *Phys. Rev.* A, **42,** 6480.

HOOGEVEEN, R. W. M., VAN DER MEER, G. J., and HERMANS, L. J. F., 1990a, *Phys. Rev.* A, **42,** 6471.

HOOGEVEEN, R. W. M., VAN DER MEER, G. J., HERMANS, L. J. F., and CHAPOVSKY, P. L., 1989b, *J. chem. Phys.*, **90,** 6143.

HOOGEVEEN, R. W. M., VAN DER MEER, G. J., HERMANS, L. J. F., GHINER, A. V., and KUŠČER, I., 1989a, *Phys. Rev.* A, **39,** 5539.

HOOGEVEEN, R. W. M., VAN DEN OORD, R. J., and HERMANS, L. J. F., 1986, *Proceedings of the 15th International Symposium on Rarefied Gas Dynamics*, edited by V. Boffi and C. Cercignani (Stuttgart: Teubner), vol. I, p. 321.

HOOGEVEEN, R. W. M., SPREEUW, R. J. C., and HERMANS, L. J. F., 1987, *Phys. Rev. Lett.*, **59,** 447.

IL'ICHOV, L. V., 1985, *Phys. Lett.* A, **111,** 289.

JACOBS, D. C., KOLASINSKI, K. W., MADIX, R. J., and ZARE, R. N., 1987, *J. chem. Phys.*, **87,** 5038.

KENNARD, E. A., 1938, *Kinetic Theory of Gases* (New York: McGraw-Hill).

KOGAN, M. N. *et al.*, 1990 (private communication).

KOGAN, M. N., BAZELYAN, A. E., and SURDUTOVICH, E. A., 1991, *Proceedings International School Lasers and Applications*, Part III, Krasnoyarsk, 1991, p. 110.

KRYSZEWSKI, S., and NIENHUIS, G., 1987, *J. Phys.* B, **20,** 3027; 1989, *Ibid.*, **22,** 3435.

LAWANDY, N. M., 1983, *IEEE J. quant. Electron.*, **19,** 1257.

LEVIN, G. A., 1981, *Pis'ma zh. tekh. Fiz.*, **7,** 439 (*Soviet Phys. Tech. Phys. Lett.*, **7,** 188).

LEVIN, G. A., and FOLIN, K. G., 1980, *Pis'ma Zh. Eksp. Teor. Fiz.*, **32,** 160 (*JETP Lett.*, **32,** 148).

LIGNIE, M. C. DE, and WOERDMAN, J. P., 1990, *J. Phys.* B, **23,** 417.

MIRONENKO, V. R., and SHALAGIN, A. M., 1981, *Bulletin of the Academy of Sciences of the USSR*, Physical Series, **45,** 87.

MÖDL, A., ROBOTA, H., SEGNER, J., VIELHABER, W., LIN, M. C., and ERTL, G., 1985, *J. chem. Phys.*, **83,** 4800.

NIENHUIS, G., 1989, *Phys. Rev.* A, **40,** 269.

NIENHUIS, G., and VAN ENK, S. J., 1991, *Ann. Phys., Leipzig*, **48,** 169.

PANFILOV, V. N., STRUNIN, V. P., and CHAPOVSKY, P. L., 1983a, *Zh. Eksp. Teor. Fiz.*, **85,** 881 (*Soviet Phys. JETP*, **58,** 510); 1983b, *Zh. Eksp. Teor. Fiz.*, **84,** 912 (*Soviet Phys. JETP*, **57,** 529).

PANFILOV, V. N., STRUNIN, V. P., CHAPOVSKY, P. L., and SHALAGIN, A. M., 1981, *Pis'ma Zh. eksp. teor. Fiz.*, **33,** 52 (*JETP Lett.*, **33,** 48).

POPOV, A. K., SHALAGIN, A. M., SHALAEV, V. M., and YAKHNIN, V. Z., 1980, *Appl. Phys.*, **25,** 347.

RAUTIAN, S. G., FOLIN, A. K., and CHAPOVSKY, P. L., 1983, *Soviet J. quant. Electron.*, **13,** 1633.

RIEGLER, H., TACKE, M., HAEFELE, H. G., and SKOK, E., 1983, *Optics Commun.*, **46,** 195.

ROLDUGIN, V. I., 1988, *Kolloidnyi Zhurnal*, **50,** 506.

VAKSMAN, M. A., 1984, *Soviet Phys. Tech. Phys.*, **29,** 681.

VAKSMAN, M. A., and GAINER, A. V., 1985, *Zh. Eksp. Teor. Fiz.*, **89,** 41 (*Soviet Phys. JETP*, **62,** 23).

VAN DER MEER, G. J., HOOGEVEEN, R. W. M., HERMANS, L. J. F., and CHAPOVSKY, P. L., 1989, *Phys. Rev.* A, **39,** 5237.

VAN DER MEER, G. J., BROERS, B., HOOGEVEEN, R. W. M., and HERMANS, L. J. F., 1992a, *Physica* A, **182,** 47.

VAN DER MEER, G. J., SMEETS, J., POD'YACHEV, S. P., and HERMANS, L. J. F., 1992b, *Phys. Rev.* A, **45,** 1303.

VIEHLAND, L. A. 1992, *Physica* A (in press).

WERIJ, H. G. C., WOERDMAN, J. P., BEENAKKER, J. J. M., and KUŠČER, I., 1984, *Phys. Rev. Lett.*, **52,** 2237.